Biol Invasions (2019) 21:1179–1195
https://doi.org/10.1007/s10530-018-1894-x

ORIGINAL PAPER

Anisotropic dispersal by the Asian longhorned beetle (*Anoplophora glabripennis*): quantifying spatial risk and eradication effort with limited biological data

R. Talbot Trotter III · Eugene Pepper · Kevin Davis · Ryan Vazquez

Received: 9 April 2018 / Accepted: 27 November 2018 / Published online: 13 December 2018

Abstract Once a breeding population of an invasive species has established in a novel environment, management efforts commonly focus on eradicating the species or limiting its spread. However, information describing the biology and behavior of an invading organism is often limited, highlighting the need to assess dispersal with incomplete information. Here we extend a previously described graph-theory-driven model of dispersal for the Asian longhorned beetle (*Anoplophora glabripennis* Motschulsky) to evaluate the impacts of three poorly documented biological and behavioral parameters on the spatial extent and distribution of dispersal risk in three breeding beetle populations under eradication in the United States. The parameters assessed include 1) whether beetles disperse from lightly/recently infested trees, 2) the presence and impact of anisotropic dispersal, and 3) the rate at which beetles emigrate from infested trees. The results suggest three key patterns. First, beetle behavior, i.e. dispersal from lightly infested trees, alters the dispersal kernel calculated for each of the infestations, though the effects of this parameter on the distribution of dispersal risk on the landscape is limited. Second, dispersal within each location was anisotropic (variable based on direction), and biases in dispersal direction varied among the three infestations. The incorporation of this anisotropy substantially altered the estimated distribution of risk within each landscape. Third, changes in the rate of beetle dispersal did not alter the perimeter of the landscape with dispersal risk but did alter the severity of risk within that perimeter. Higher rates of dispersal result in the need to mitigate larger portions of the landscape to achieve a given probability of eradication. These tools can aid in quantifying and comparing dispersal risk under varying assumptions of dispersal, and may help prioritize research on biological and behavioral parameters to facilitate management and eradication.

Keywords Spatial risk · Dispersal kernel · Insect dispersal · Graph theory · Eradication effort

Electronic supplementary material The online version of this article (https://doi.org/10.1007/s10530-018-1894-x) contains supplementary material, which is available to authorized users.

R. T. Trotter III (✉)
Forest Service, Research and Development, Northern Research Station, United States Department of Agriculture, Hamden, CT 06514, USA
e-mail: rttrotter@fs.fed.us

E. Pepper · K. Davis · R. Vazquez
Massachusetts Asian Longhorned Beetle Eradication Program, Animal Plant Health Inspection Service, United States Department of Agriculture, Worcester, MA 01606, USA

Introduction

While species invasions create challenges for natural resource management, they also provide opportunities to study the fundamental processes of establishment and spread, information that can benefit management and eradication efforts (Liebhold and Tobin 2008). However, allowing invasive organisms to freely reproduce and disperse is typically antithetical to management efforts focused on rapid quarantine and eradication. As a result, studies of dispersal by invasive species are often limited to studies in the species' native range, or to information that can be collected in concert with eradication programs. The Asian longhorned beetle (*Anoplophora glabripennis* Motschulsky) is an example of this scenario.

A. glabripennis is native to China and the Korean Peninsula (Wu and Jiang 1998; Peng and Liu 1992; Lingafelter and Hoebeke 2002; Williams et al. 2004a) but has been moved to novel locations as a stow-away in solid-wood packing material such as the pallets and crates used in international shipping (Haack et al. 2010). Its broad host-range (at least 15 genera including *Acer*, *Populus*, and *Salix*), proven ability to survive shipment, and ability to damage tree health and structure make this a high-risk species (Lowe et al. 2000). Prior to its discovery in New York City in the United States in 1996 (Haack et al. 2000), research on this beetle was primarily focused on its impacts on exotic tree species planted in China as part of the Three North Shelter Forest Program (Yan and Qin 1992). Since its discovery in the U.S., breeding populations of the beetle have been found in numerous countries including Austria, Belgium, Canada, Finland, France, Germany, Italy, the Netherlands, Switzerland, Turkey, and the United Kingdom. Due to the risk posed by this species, countries including the U.S., Canada, and members of the European and Mediterranean Plant Protection Organization (EPPO, https://gd.eppo.int/taxon/ANOLGL/documents) have adopted polices of quarantine and eradication.

The eradication of Asian longhorned beetle populations depends on identifying and destroying individual infested trees, however finding infested trees can be challenging. The majority of the life-history of the beetle is spent within the cambium and xylem of the host tree making the beetles themselves difficult to detect. While the development of traps and lures has shown some promise (Meng et al. 2014; Nehme et al. 2014), operational traps and lures are not yet available. These limitations have led eradication programs to depend on visual surveys to identify infested trees.

Visual surveys are based on identifying the oviposition pits and exit holes adult beetles leave on host trees. Gravid females chew pits in the bark of host trees to insert eggs into the phloem, leaving a distinctive bark wound. After hatching larvae proceed through three instars in the cambium, then move to the xylem to proceed through a variable number of instars (Keena and Moore 2010; Trotter and Keena 2016). Beetles then pupate in a chamber a few centimeters under the bark where they eclose, sclerotize, and chew through the wood to emerge, leaving a nearly perfectly circular exit hole $\sim$ 1 cm in diameter. These oviposition pits and exit holes provide the visual indications of infestation used by survey personnel to identify infested trees. Surveys are typically conducted from the ground using binoculars, by tree climbers, or using bucket trucks and aerial lifts. Once an infested tree is identified, it is felled and destroyed by chipping (USDA 2014b).

Although visual surveys have been used to successfully eradicate populations of *A. glabripennis* in the urban landscapes of Chicago, Illinois (USDA 2008), Linden, New Jersey (NJDA 2013), and Boston, Massachusetts (USDA 2014a), the approach is time-consuming, labor-intensive, and costly. Without detailed data and models of beetle dispersal, eradication programs have identified survey priorities using fixed radius buffers around known infested trees, and have not had access to cost–benefit analyses to prioritize survey distances, directions, and intensities. In larger infestations such as those around Worcester, MA, and Bethel, OH, thousands of infested trees can be distributed within millions of host trees over hundreds of square kilometers. In landscapes like these, there is a clear need to optimize search strategies by basing them on patterns of beetle dispersal.

Past efforts to quantify beetle dispersal

When the infestation in New York City was identified in 1996 data describing the behavior and dispersal of *A. glabripennis* were not readily available. To fill this knowledge gap Smith et al. (2001, 2004) conducted large-scale capture-mark-recapture studies in the beetle's native range in China. These experiments involved the capture and release of 16,511 and 39,960

individual beetles (respectively), with recapture locations radiating from the point of release to 600 and 1080 m. The results of these studies indicated 98% of the re-captured beetles traveled less than 560 and 920 m, providing preliminary estimates of beetle dispersal kernels. However as the authors discussed, even with the large-scale sampling and the recapture of 188 and 395 beetles, the rare long-distance dispersal events that make up the tail of the dispersal kernel may not be documented, and the study was limited to quantifying beetle dispersal in a broadly established native population.

Subsequent studies provided additional data by evaluating dispersal in invaded landscapes. Using the records of beetle activity left in tree rings, Hull-Sanders et al. (2017), Straw et al. (2016), and Turgeon et al. (2015) reconstructed patterns of beetle establishment and spread in isolated populations in the United States, England, and Canada, respectively. These three populations revealed shared patterns including relatively slow population growth rates, low dispersal rates, and indications the beetle tends to remain on its natal tree. These studies have provided novel information on the process of population establishment and spread, however the methods used by these studies depend on the dissection of individual trees to date beetle damage. In populations where thousands of trees are infested, this approach may not be scalable.

More recently a quantitative method suitable for larger infestations has been developed by Favaro et al. (2015). Using semiannual surveys of a 5600 ha landscape that included 466 infested trees and > 12,000 uninfested trees, Favaro et al. (2015) developed a generalized linear model based on a cumulative distribution function to quantify risk of beetle attack as a function of the distribution of infested trees. This method offers a number of advances including the ability to quantify spatial variation in risk and a method suitable for larger infestations. However, the approach includes some limitations including the need for complete annual surveys and the assumption of a univoltine life-history for the beetle. Since the publication by Favaro et al. (2015), recent work by Trotter and Keena (2016) suggests this univoltine assumption may be violated, and on landscapes with millions of host trees, complete annual surveys may not be feasible.

A fourth approach developed by Trotter and Hull-Sanders (2015) offers a method to assess beetle dispersal within large infestations. Using a graph-theory driven model this method provided a way to develop dispersal kernels for *A. glabripennis* within a 284 km^2 landscape with more than 7000 infested trees around Worcester, MA, USA. This approach is well suited to large infestations (for which infested tree records are available) and does not depend on complete annual surveys or voltanism assumptions. This method also offers flexibility in dispersal assumptions and can be used to evaluate the effects of poorly known parameters, such as the potential for newly or lightly infested trees to serve as sources of dispersing beetles (Trotter and Hull-Sanders 2015). This study however included a number of significant limitations. While it assessed the role of newly infested trees in shaping the dispersal kernel and determining the perimeter of the landscape with dispersal risk, this study did not assess, 1) the distribution of risk within the perimeter of dispersal risk, 2) the role and importance of anisotropic dispersal and variation in dispersal rates, or 3) the generality of the findings beyond this single infestation.

Here we describe an extension of this graph-driven method to address these issues and to provide an improved understanding of *A. glabripennis* dispersal by evaluating the role of poorly understood dispersal parameters on the spatial distribution of risk on the landscape. Using this extended tool, we address four primary questions. First, past work indicates the inclusion or exclusion of beetle dispersal from lightly infested trees plays a limited role in determining the perimeter of dispersal risk (Trotter and Hull-Sanders (2015), but does this unknown behavior alter the distribution or intensity of risk within this perimeter? Second, is there evidence of anisotropic dispersal within and among three invasive ALB populations, and does this anisotropy substantially alter the distribution and intensity of dispersal risk? Third, does variation in dispersal rate (bracketed by values from the published literature) impact the distribution or intensity of dispersal risk on the landscape? Finally, how do combinations of these parameters (hereafter referred to as scenarios) alter the relationship between the level of management effort applied to the landscape, and overall probability of eradication?

Methods

Data source and content

Analyses of beetle movement and spatial risk were conducted for regions within the United States around the known Asian longhorned beetle infestations in Worcester, MA, Bethel, OH, and on Long Island, New York. Each of these areas are under eradication management plans operated cooperatively by the United States Department of Agriculture (USDA) Animal and Plant Health Inspection Service (APHIS) Asian Longhorned Beetle Eradication Program, and the Massachusetts Department of Conservation and Recreation (Mass DCR), the Ohio Department of Agriculture (ODA), or the New York Department of Environmental Conservation (NYDEC), respectively. Each of these federal-state cooperative efforts is referred to as a Cooperative ALB Eradication Program which operates under the field guidelines described in USDA (2014b). Briefly summarized, the eradication programs are based on visual surveys conducted by ground personnel using binoculars, tree climbers, and bucket-truck operators who search individual trees for exit holes and oviposition pits (USDA 2014). Surveys are conducted on a zone-by-zone basis (with zones being defined locally by programs), with the goal of surveying each zone multiple times to ensure all infested trees are identified and destroyed. Due to the sizes of the regulated areas and the numbers of trees involved, annual surveys typically cover only a portion of the total area of interest and multiple years may pass between surveys at a given location. When infested trees are located, information including the tree's location (latitude and longitude), diameter at breast height, level of infestation, genus and (when available) species is documented by the local Cooperative ALB Eradication Program using hand-held geographic information systems (Intramaps Roam^{TM}). The level of infestation is recorded as a categorical value, with trees being assigned to category A, B, C, or D. A-level trees are trees which have oviposition pits but lack exit holes, B, C, and D trees are those with 1–10, 11–100, or > 100 exit holes, respectively. Because each exit hole represents the addition of a single adult to the population, the infestation category serves as a proxy for the size of the adult beetle population produced by each tree. The ALB Eradication Program data used for the Worcester, MA, Bethel, OH, and Long Island, NY locations were compiled on January 11th, 2018, January 9th, 2018, and January 10, 2018, respectively. QA/QC procedures followed the QA/QC protocols in place for the Cooperative ALB Eradication Programs (USDA 2014a, b).

Analysis and model overview

Within these analyses, the distribution of risk of infestation by the Asian longhorned beetle on the landscape is estimated using a process with four basic steps summarized here and described in greater detail below. First, dispersal events on the landscape are inferred by identifying connections among infested trees representing beetle dispersal events using the method described in Trotter and Hull-Sanders (2015) under two sets of assumptions (Strict and Relaxed). Varying these assumptions provides a method to assess the importance of the propensity of beetles to disperse from lightly infested trees, a component of beetle behavior for which limited data is available. Second, the inferred beetle movement vectors are divided into bins based on the vector direction. These bins of vectors are then used to generate direction-specific dispersal kernels. Third, the number of adult beetles produced by each of the infested trees on the landscape is inferred based on the infestation level, and the number of dispersing beetles is estimated using multiple published and unpublished dispersal rates. Fourth the dispersal kernels (either directional or generalized) are applied to the locations of each of the infested trees on the landscape to estimate the probability that at least one beetle from the tree has dispersed to each given ha on the landscape, based on the direction and distance to the infested tree. Within this study, the landscape is divided into a 1 ha grid. This process is repeated for each of the known infested trees on the landscape, and the probabilities for each ha are compiled to estimate the overall probability that at least one beetle from any tree has arrived and established within a given ha, based on the distribution and level of infestation of all known infested trees. These steps were accomplished computationally using a suite of scripts built in MatLab (R2017a v9.2.0.538062) which are available as raw scripts or a single stand-alone executable file (ALB_Risk_v1.exe).

Early in the eradication programs, the locations of trees were documented using the centroids of the

properties on which they were found. The result is a subset of trees found early in the program which include identical locations (i.e. the property centroid). Triangulation requires unique locations, and so these positions were adjusted by shifting them eastwards in 0.1 mm increments to insure all inter-tree vectors were compiled, and to ensure trees of different infestation levels but with identical locations were included. This allows computation of spatial relationships while introducing variation in location at a scale that is inconsequential to the meter-scale analyses. These short, synthetic vectors were removed in tests for biases in dispersal direction to avoid artificial weighting of dispersal distances.

Identifying adjacencies among Infested trees (step 1): the role of dispersal behavior

Beetle movements between trees are inferred by identifying adjacencies among trees. These adjacencies are defined using sets of rules regarding assumed beetle movement. For the following analyses, the rulesets used include the Relaxed and Strict rules as described in Trotter and Hull-Sanders (2015). Briefly summarized, the Strict rule assumes that only heavily infested trees can serve as the source of dispersing beetles, thus dispersal vectors must originate from C and D level trees. Within the Relaxed assumptions, all trees with exit holes can serve as the source of a dispersal vector. In both cases, trees are assumed to have been infested by beetles originating from the closest source tree which has a level of infestation which is higher (and presumably older) than the tree receiving the beetles. Trees are assumed to have been infested only once, though individual trees can serve as the source of beetles for multiple trees. These tree adjacencies represent dispersal and establishment vectors (v) for individual beetles and are defined by distance ρ (in m) and direction θ (in radians).

Direction specific dispersal kernels (step 2): quantifying anisotropy

Dispersal vectors were tested statistically for anisotropy within locations using Kuiper's test, which is similar to a Kolmogorov–Smirnov test that is not sensitive to variations in orientation (rotation invariant). The distribution of dispersal directions was compared with a null model based on a uniform distribution. Comparisons among locations were made using a Kolmogorov–Smirnov test. To produce direction-specific dispersal kernels, dispersal vectors (v) were sorted by ϑ and placed in n_ϑ bins with an angular size β. Values of β are limited to those which, when divided into 2π produce integers, i.e. all bins are required to be the same size, such that:

$$\frac{2\pi}{\beta} = n_\vartheta | n_\vartheta \; is \; integer \tag{1}$$

Within the following analyses, dispersal kernels were evaluated using $\beta = 0.5236$ rad, equal to direction bins of 30°, with the edge of the first bin along the eastern axis (bearing 90°). A single 360° bin was also used to produce a non-directional dispersal kernel.

To produce the dispersal kernels, the dispersal vectors (ρ) within each of the directional bins (β_ϑ) were sorted by length and indexed sequentially. The percentile for each vector v is then calculated using:

$$Pt_{v,\beta\vartheta} = \frac{i_{(v,\beta\vartheta)}}{n_{\beta\vartheta}} \tag{2}$$

where $Pt_{v,\beta\vartheta}$ is the percentile of vector v in β_ϑ, $i_{(v,\beta\vartheta)}$ is the index of vector v, and $n_{\beta\vartheta}$ is the total number of distance vectors in direction bin β_ϑ. Plotting the values of Pt for each vector as a function of vector length yields empirical dispersal kernels. Graphical representations of dispersal kernels are shown with percentile values plotted at 0.001 increments (Figs. 2, 3, 4 and 5).

Parameterizing dispersal rates (step 3): estimating the number of dispersing beetles

Calculating the probability of beetles arriving at a given location requires knowledge or assumptions regarding the number of beetles dispersing from a given tree. Because only females can initiate new infestations, we focus here on identifying the number of dispersing female beetles emigrating from each tree. For simplicity we assume all female beetles to be mated. Generally, the number of female beetles which emigrate from a tree is expected to be a function of the total number of adult beetles on the tree, the proportion of the population which is female, and the rate at which beetles emigrate, such that:

$$n_{EF} = n_A * r_F * r_E \tag{3}$$

where n_{EF} is the number of emigrating females produced by a tree, n_A is the total number of adult beetles produced by a tree, r_F is the proportion of the adult population which is female, and r_E is the generalized rate of emigration.

Within these analyses, the total number of adult beetles produced by a tree (n_A) is derived from the data collected by the Cooperative Asian Longhorned Beetle Eradication Programs. The programs assign trees to one of four infestation categories based on the type and quantity of damage, such that A-level trees are those which have oviposition pits, but no exit holes, and B, C, and D-trees have 1–10, 11–100, and > 100 exit holes, respectively. Each exit hole represents the addition of an adult beetle to the population, and for the purposes of these analyses, we assume that both B and C-level trees have produced the maximum number of adult beetles (10, and 100) for their respective categories, with the understanding that this approach assumes a *worst-case-scenario* regarding the number of dispersing beetles. D level trees are uncommon on the landscape, but frequently have between 200 and 400 exit holes, and so here we apply the extreme value of 400. A-trees represent a unique challenge in estimating the number of emigrating adults expected. While A-trees lack exit holes and functionally do not add adult beetles to the population, discrete isolated pockets of A-level trees are common on the landscape. Because these clusters of trees are likely the result of a single female infesting multiple adjacent trees (rather than the less parsimonious assumption multiple females which dispersed in the same direction for the same distance at the same time to infest adjacent trees), the movement of female beetles from one newly produced A-tree to another functionally makes each A-tree a potential source for a dispersing beetle. To accommodate this, we assume that each A-level tree produces a single beetle, noting that the application of Eq. 3 to A-level trees results in each tree yielding a small fraction of a dispersing adult female.

The proportion of the adult beetle population which is female (r_F) is captured by the sex ratio of the population, and although data on the sex ratio of the Asian longhorned beetle is limited two previous studies provide guidance. Bancroft and Smith (2005) conducted population surveys in the beetle's native range, and with a sample of nearly 1500 beetles found a slight male bias with a male: female ratio of 1.14. In a laboratory study conducted by Melody Keena (personal communication), nearly 1000 beetles were reared from cut, field collected wood which was stored in a constant temperature environment. This study also found a population with more males numerically, however, an analysis of the data did not provide statistical support for a sex ratio different from 1:1. Taken together, these data suggest that populations of the Asian longhorned beetle may include a slight male bias, but based on the limited bias observed by Bancroft and Smith (2005), and the lack of a bias found by Keena, the use of a 1:1 sex ratio may be a reasonable simplifying assumption. The potential for this bias however highlights the need for additional work on this issue. We also note that using a 1:1 ratio, if there is a male bias, would tend to slightly overestimate the number of dispersing females by overestimating the number of females in the population. This would have the effect of again assuming a worst-case-scenario.

We based emigration/dispersal rates (r_E) on behavioral observations made in both field and laboratory settings. While dispersal behavior is likely driven by complex interactions between intrinsic and extrinsic factors such as beetle age, gender and size, host condition, host species, beetle density, temperature, and wind-speed, as well as stochastic events such as disturbance, limited data is available on the propensity of an ALB to take flight and disperse from its natal tree. Previous work has suggested that, while the beetle is capable of long-distance flight (Smith et al. 2001, 2004; Trotter and Hull-Sanders 2015; Javal et al. 2017; Lopez et al. 2017), beetles may commonly remain on their natal tree until the tree has been heavily utilized (USDA 2014), suggesting rates of emigration may generally be low.

To bracket dispersal rates, we used available laboratory and field assessments of beetle dispersal behavior to estimate the upper and lower limits of dispersal rates. At the lower end, laboratory assessments of flight behavior found that the initiation of flight by adults is influenced by host condition and abiotic factors such as wind-speed and temperature (Keena and Major III 2001), with female dispersal rates as low as 5%. These data suggest that, under suitable conditions, as few as 1 in 20 females may be expected to leave the natal tree. However, it is important to note that a laboratory setting lacks many

of the cues and disturbances associated with field conditions, consequently the observed 5% may underestimate natural dispersal rates.

Two studies have documented dispersal behavior under field conditions. In the first study, Williams et al. (2004b), used harmonic radar to track the movements of individual beetles in a willow stand within the beetle's native range in China. Of the 21 females in the study, 15 remained on the tree on which they were first trapped and released, indicating 29% of female beetles may be expected to take flight and disperse. While this study benefited from a naturalized field setting, the use of the harmonic radar and tags involved tracking and re-capturing the beetles an average of 2.8 times over a 9–14 day period, and the repeated disturbances associated with capture and release may have impacted beetle behavior. In a second field study, Bancroft and Smith (2005) found higher levels of dispersal, with 62% of the studied beetles moving from the tree on which they were released, a rate similar to $\sim$ 60% observed in the laboratory by Keena and Major (2001) when beetles were on unsuitable host (dead wood). This study also found an increase in dispersal associated with increased beetle density. At the peak of the observed emergence within the study, beetles were emerging at a rate of 0.25 beetles/tree/day. Because these densities and emergence rates are higher than those typically found in recently infested landscapes, the Bancroft and Smith (2005) and Keena and Major (2001) data may overestimate the natural tendency of beetles to disperse in newly established populations where population densities are lower, and trees are alive and minimally infested. Collectively, the lower dispersal rate (r_E) of 5% may underestimate dispersal, while the upper rate of 62% may overestimate it, however, these values provide outer brackets for actual dispersal rates under field conditions.

Using the above parameters in Eq. 3 results in the production of 0.025, 0.25, 2.5, and 10 dispersing females (n_{EF}) for A, B, C, and D-level trees under the low (5%) dispersal assumption, and 0.31, 3.1, 31, and 124 dispersing females under the high (62%) dispersal assumption.

Spatial estimates of dispersal probability (step 4)

If the dispersal kernel (whether directional or non-directional) is separated into distance bins (β_ρ) of size ρ, the probability of a beetle dispersing and arriving within distance bin d is:

$$P_d = Pt_d - Pt_{d-1} \tag{4}$$

where P_d is the probability of a beetle landing within distance bin d, Pt_d is the cumulative percentile of dispersal events including those in distance bin d, and $Pt_{d\text{-}1}$ is the cumulative percentile of dispersal events shorter than distance bin d. Spatially, the values for P_d can be represented as a series of rings around the infested tree, with values representing the probability of a beetle arriving within the ring. To determine the probability of a beetle arriving at a given location, the landscape is rasterized and the location of each pixel is defined by its center. The area of each ring is then divided by the area of a single pixel to determine the nominal number of pixels within each ring, and the total probability of a beetle arriving within the ring is divided by the number of pixels to provide a pixel-specific probability of beetle arrival (P_{ba}) for a pixel with a center within a given distance bin. For these analyses, the size of the distance bins (β_ρ) and probability rings, and the size of the raster pixels were set to 100 m. As the pixel size equals 1 hectare, raster locations are hereafter referred to as hectares, for simplicity.

To simplify later calculations, the probability of a single beetle's presence is converted to the probability of beetle absence such that:

$$P_{ba} = 1 - P_{bp} \tag{5}$$

where P_{ba} equals the probability of beetle absence and P_{bp} is the probability of beetle presence. The probability of beetle absence is then raised to the power of the number of beetles dispersing from a given tree, such that the overall probability that no beetles have arrived at a given hectare, given n_{EF} female beetles dispersing from a given tree, is:

$$P_{ba}^{n_{EF}} \tag{6}$$

The probability of a dispersal event occurring within each direction bin is adjusted based on the proportion of events observed in the data to preserve directional biases. In the case of both the directional and non-directional dispersal estimates the result of the above is a rasterized landscape in which the value for each hectare describes the estimated probability of beetle absence, based on the location and level of

infestation of a single tree. This process is repeated for each tree-hectare pair, and the product of the probabilities of beetle absence for each hectare produces the cumulative probability of beetle absence at a specified hectare given the locations and levels of infestation for all known infested trees. It is important to note however, that this assumes spatial independence among hectares and dispersing female beetles, and the implications of this assumption remain unknown. Landscape-scale probabilities were calculated for each hectare within a 40 × 40 km landscape. The inclusion of the 160,000 hectares was adequate to capture all of the hectares for which the calculated probability of beetle presence was > 0, for each of the three infestations.

Summarizing landscape risk by quantifying the effort required for eradication

To assess the impact of the three study parameters (propensity to disperse from lightly infested trees, anisotropic dispersal, and dispersal rates) on the distribution and intensity of risk on the landscape, eradication effort curves were calculated for each combination of parameters. Eradication effort curves estimate the number of hectares which must be mitigated to achieve a given probability that the beetle has been eradicated from the landscape. In these analyses, we assume that once a hectare has been mitigated, the probability of beetle presence is reduced to zero. If all of the hectares for which the risk of beetle presence is greater than 0 are ranked from highest to lowest, and hectares are mitigated in the order in which they are ranked, then the probability that none of the remaining hectares are infested can be calculated as the product of the probabilities that each of the remaining hectares are not infested, such that:

$$P_{E,n} = P(B_a)_{n-1} * P(B_a)_{n-2} \cdots \quad (7)$$

where $P_{E,n}$ equals the probability of eradication for the entire landscape, given the mediation of risk on the n highest risk hectares, and $P(B_a)_{n-1}$ equals the probability of beetle absence in the remaining hectare(s). Graphing the probability of eradication as a function of the number of hectares mitigated produces an eradication probability/effort curve. Comparison of the curves for each of the scenarios provides a way to compare the effect of each combination of parameters on the relative quantity and intensity of risk on the landscape.

Results

Variation in dispersal among infestations and dispersal behaviors

At the time the survey data for these analyses were compiled (January 2018) the Asian longhorned beetle infestation centered in Worcester, MA included 10,301 individually documented infested trees (note this does not include trees deemed high-risk, or individual infested trees which were removed as part of whole-host removal efforts) while the database of infested trees used for Bethel, OH included nearly twice as many with 19,004 (51 infested trees in two small isolated satellite infestations known to be the result of fire wood movement were excluded). The beetle population under eradication on Long Island, which likely represents a large satellite infestation from the previously managed area around New York City contained 840 infested trees. Although the number of infested trees varied substantially among these three locations there is not an obvious link between the number of trees and the size of the infested landscape. Figure 1 represents the inferred dispersal vectors in each of the three infestations set to the same spatial scale, and suggests the Massachusetts population nominally infests a landscape of $\sim$ 260 km^2 (based on east–west by north–south range), while the infestation in Ohio nominally covers $\sim$ 80 km^2, despite Ohio including nearly twice as many infested trees. The Long Island infestation is similarly sized with $\sim$ 65 km^2, though the number of infested trees on Long Island is an order of magnitude smaller. Currently, the landscape characteristics that structure the relationship between the number of infested trees and the size of the infested landscape remain to be identified.

The dispersal kernels produced by applying the vectors from Fig. 1 to Eq. 2 demonstrate two patterns. First, dispersal distances and probabilities vary among the three locations. Figure 2 provides the composite (non-directional) dispersal kernels for each of the locations under assumptions of Strict and Relaxed dispersal behavior. Populations with lower curves

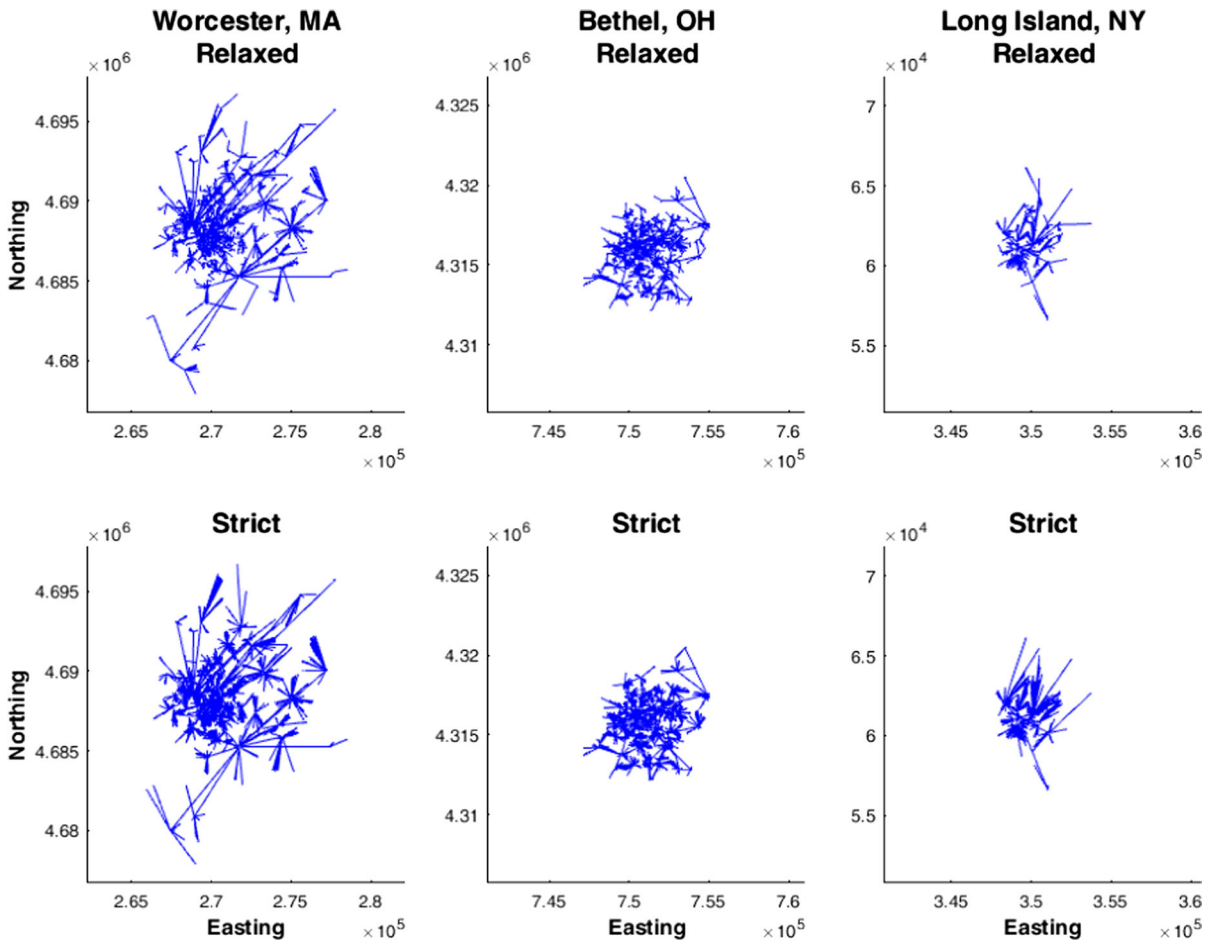

Fig. 1 Although the numbers of infested trees varies substantially among the infestations, there seems to be little connection between the number of trees infested, and the spatial distribution of the infestation. Maps shown provide the estimated dispersal vectors based on Relaxed assumptions, in which beetles are assumed to disperse from all infested trees, and Strict assumptions in which dispersal is limited to trees with moderate to heavy infestations

have a larger portion of the population which will disperse as far as, or farther than the specified distance compared to populations with steeper/higher curves. A comparison of the three locations shows that the highest proportion of long-distance dispersal vectors were found on Long Island (dotted line), while the lowest proportion was found in Bethel, OH. The end points of the curves represent the longest observed dispersal distances, and the curves show these maximum distances varied among the locations. The longest dispersal distances occurred in Worcester, MA, while the population in Long Island, NY had the shortest maximum dispersal distance.

The second pattern shown by the dispersal kernels is that changes in beetle behavior produced consistent changes in dispersal distances and probabilities across all three locations, despite the difference in the sizes of the infestations. Under Strict dispersal assumptions the frequency of long-distance dispersal events increased within each of the three infestations. The mechanism driving this is likely the reduction in the number of potential source trees and the resulting increase in the typical inter-tree distance between source and destination trees. As previously discussed both here and in Trotter and Hull-Sanders (2015) the geographic patterns associated with Strict dispersal are likely less parsimonious than those produced by Relaxed assumptions.

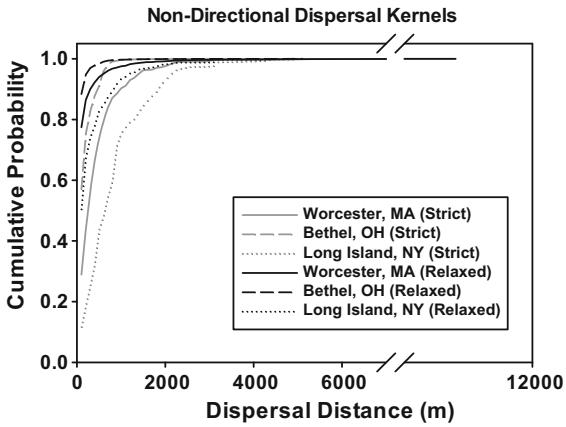

Fig. 2 Among the three studied infestations (shown in solid, dashed, and dotted lines), beetles in the Long Island population had a higher probability of dispersing to distances up to ~ 4000 m compared to the other two populations. However, beetles in Long Island also had the shortest maximum dispersal distances as demonstrated by the ends of the curves. Shifting from Strict to Relaxed dispersal behaviors (grey and black lines, respectively) resulted in reduced probabilities of long-distance dispersal event in all three populations

Dispersal distances, probabilities, and anisotropy

Within each of the three infestations (under both Strict and Relaxed dispersal), dispersal vectors occurred in all directions (Fig. 1), however the distributions of dispersal directions were not uniform. Each of the three locations exhibited significant directional bias (Table 1), and these asymmetrical distributions varied among locations and under changes in assumed dispersal behavior (Table 2).

To assess this anisotropy dispersal vectors were grouped into 30° directional bins to produce direction-specific dispersal kernels. Figure 3 provides an example of these dispersal kernels for Worcester, MA. To simplify the graphical interpretation of these curves they can be plotted in three dimensions, with each curve oriented in the direction it represents to produce a dispersal kernel surface such as the one shown in Fig. 4. Note that the vertical axis has been limited to the 90th–100th percentile dispersal events to emphasize directionality. Rotating this surface so it is viewed down the vertical axis produces a graphic that shows the spatial distribution of dispersal probabilities around the point of origin (the location of the source tree) as shown in Fig. 5. These dispersal kernel surfaces describe the variation in dispersal probabilities and directionality among the three infested landscapes, and statistical analyses (Table 2) indicate each of these is unique. Within Worcester, MA dispersal was biased toward the northeast and southwest while in Bethel, OH long-distance dispersal was biased towards the southeast and northwest. In Long Island dispersal was biased primarily towards the northeast, with some rare long distance dispersal events towards the south-southwest. The maximum dispersal distances shown in the dispersal kernels (Fig. 2) are demonstrated in these dispersal kernel surfaces by the outer perimeter of the surface area, and each figure is rendered at the same scale. The open areas within the center of each surface represent the lower 90th percentile of dispersal events, and the asymmetry of these spaces show that directional biases are evident at shorter dispersal distances, though these biases may differ from those at longer distances.

Table 1 Within each of the three populations, and across both Strict and Relaxed assumptions of beetle dispersal behavior, dispersal vectors deviated significantly from a random, uniform pattern based on Kuiper's test

	p	Test statistic
Worcester relaxed	< 0.01	4.2524
Bethel relaxed	< 0.01	4.1106
Long island relaxed	< 0.01	2.9215
Worcester strict	< 0.01	11.6026
Bethel strict	< 0.01	8.2396
Long island strict	< 0.01	5.8485

The effects of dispersal behavior, anisotropy, and rate on the distribution of dispersal risk

The application of the dispersal kernel surfaces to the landscape using the locations of each of the known infested trees (Eqs. 2, 4–6) results in a composite estimate of the risk of dispersal on a hectare-by-hectare basis. Examples of these hectare-level risk estimates are shown in Fig. 6 under the assumptions of directional dispersal (risk shown in color), and non-directional dispersal (shown in white). To facilitate comparisons among the scenarios (combinations of behavior, directionality, and dispersal rate), the effort required to achieve a given probability of landscape-level eradication was calculated (Eq. 7), with effort

Table 2 The distribution of the anisotropic dispersal varied significantly both among the infestations, and within infestations under assumptions of Strict and Relaxed dispersal behavior

	Bethel relaxed	Long island relaxed	Worcester strict	Bethel strict	Long island strict
Worcester relaxed	p = 0.0001892	p = 0.017	p < 0.00001	p < 0.00001	p < 0.00001
	D = 0.026957	D = 0.055568	D = 0.048095	D = 0.05549	D = 0.12399
Bethel relaxed		p = 0.0001953	p < 0.00001	p < 0.00001	p < 0.00001
		D = 0.076173	D = 0.073149	D = 0.046669	D = 0.12769
Long island relaxed			p = 0.003056	p < 0.00001	p = 0.0001366
			D = 0.064788	D = 0.095549	D = 0.10699
Worcester strict				p < 0.00001	p < 0.00001
				D = 0.074479	D = 0.15021
Bethel strict					p < 0.00001
					D = 0.16275

Differences based on dispersal behavior however may play a limited role in structuring the distribution of risk on the landscape (Figs. 5 and 6)

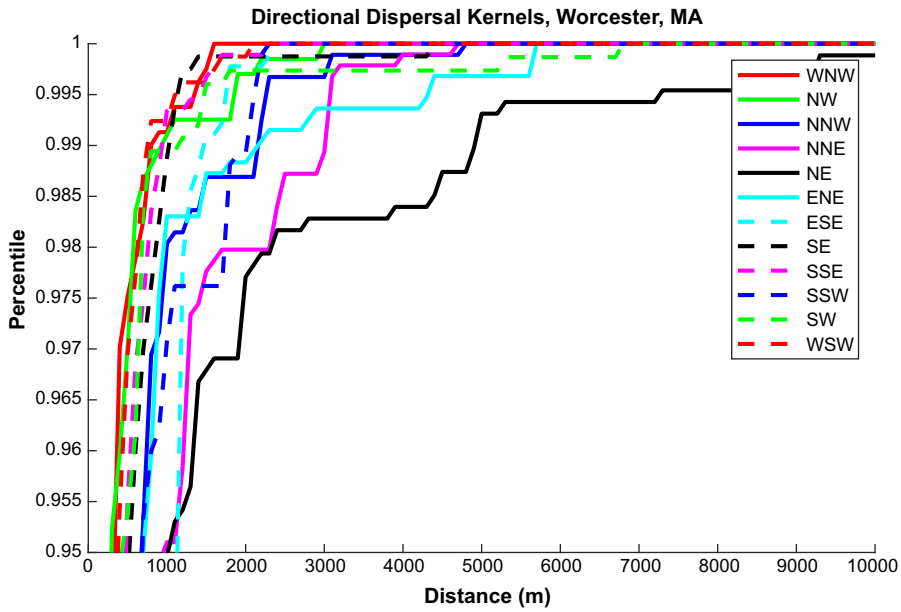

Fig. 3 The curves represent the dispersal kernels for vectors grouped in 30° bins using the Worcester, MA infestation under assumptions of Relaxed dispersal behavior. The variation in the shapes of the curves demonstrates the anisotropic dispersal found in each of the three infested landscapes (statistical comparisons shown in Table 1). The patterns of anisotropy among the locations varied (not graphically shown), and between dispersal behaviors (statistical comparisons shown in Table 2)

being measured as the total number of hectares on which risk has been mitigated (Fig. 7). The results show several patterns. First, although dispersal kernels were affected by changes in the assumed behavior of beetles as shown in Fig. 2, this variation had a limited effect on the intensity and distribution of risk on the landscape, as shown by the small horizontal shift between the Strict (solid line) and Relaxed (dashed line) eradication curves.

In contrast, the inclusion of dispersal directionality had a large effect on the quantity and distribution of risk on the landscape (Fig. 7). Non-directional dispersal kernels (shown in grey) are shifted substantially to the right of their directional counterparts (shown in black), indicating that, with other parameters held constant, a failure to include anisotropy results in an increase in the apparent risk on the landscape and a concomitant increase in the expected effort required to achieve a given probability of eradication. This

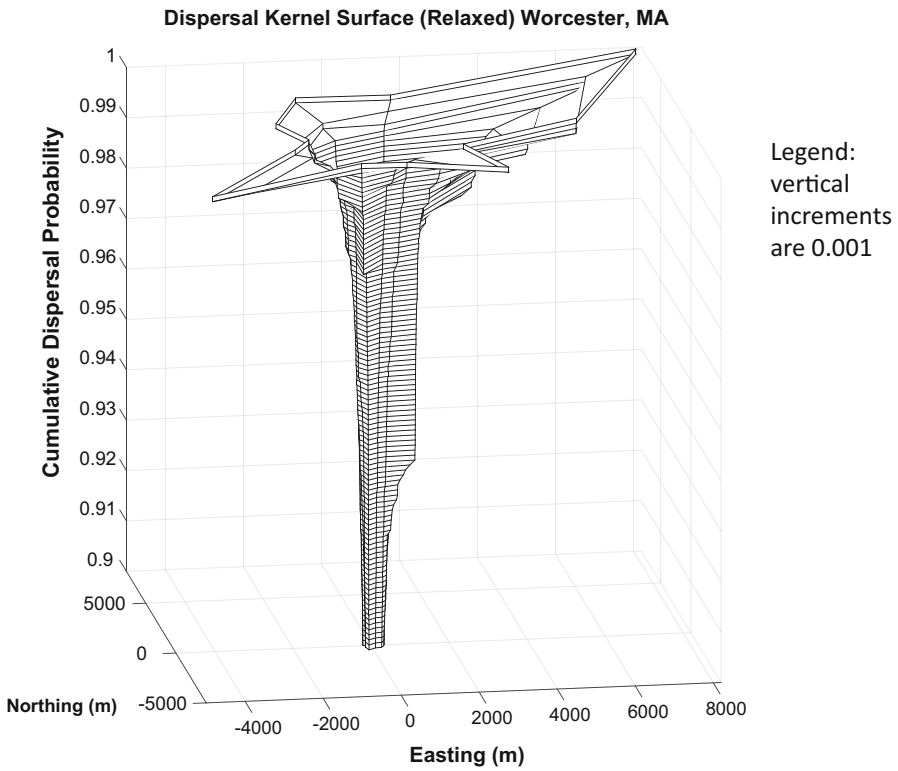

Fig. 4 Orienting each of the directional dispersal kernels shown in Fig. 3 according to its compass bearing produces a dispersal kernel surface such as the one shown above

increase in apparent risk is the result primarily of the extension of dispersal events in a 360° radius around each infested tree, rather than limiting them only to the combinations of distance and direction observed.

The largest changes in risk distribution and intensity were the result of changes in beetle dispersal rates. An increase in the dispersal rate produces a higher per-hectare risk, and the result is an increase in the number of hectares that must be mitigated to achieve a given overall probability of eradication. It is worth noting that the changes in the quantity of risk on the landscape shift, without altering the perimeter of the at-risk landscape. The outer perimeter of risk is determined by the maximum observed dispersal distance (i.e. the end point of the dispersal kernel), which does not change with changes in dispersal rate.

Conclusions and discussion

Calculating the risk of dispersal to a specified point on the landscape requires information about the dispersal behavior and ecology of the species, however for many invasive species this information is limited. Here we have extended a previously described method to develop dispersal kernel surfaces for three invading populations of the Asian longhorned beetle with variations in three poorly documented dispersal parameters, and have applied the resulting dispersal kernel surfaces to the landscape to quantify the distribution and intensity of dispersal risk. The results provide two key findings.

First, the analyses show that patterns of dispersal vary among the three studied infestations, and suggest patterns of risk may not be adequately captured using a standardized fixed dispersal distance. As the reconstruction of dispersal events shows (Figs. 1, 3, 4, 5, 6 and 7), there is substantial bias in dispersal direction within each of the studied infestations, and failure to include this bias inflates the size of the at-risk landscape. These data also suggest the biases in dispersal direction vary substantially among the locations, indicating site-specific risk estimates should be based on local patterns of dispersal.

Although this study has documented anisotropic dispersal in three Asian longhorned beetle populations, the mechanisms that drive these differences remain to be identified. A previous stand-scale study

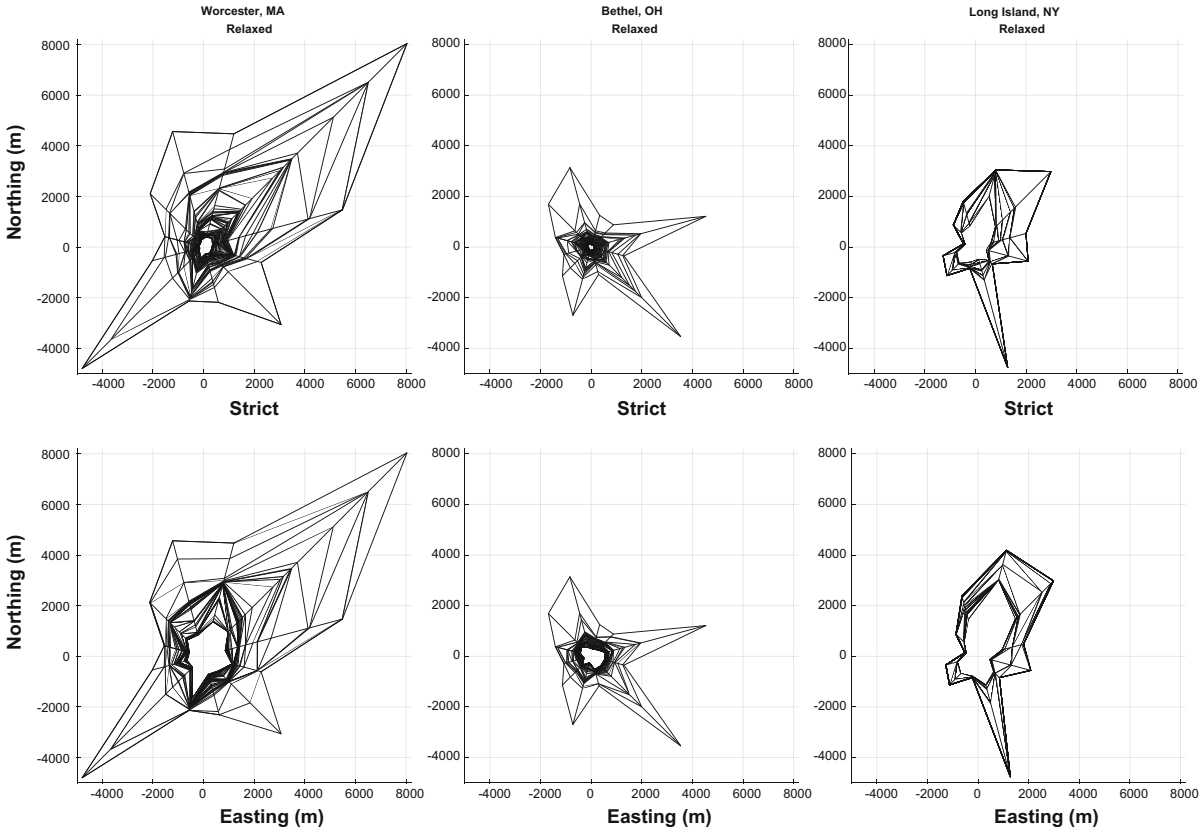

Fig. 5 Rotating the dispersal kernel surface such as the one shown in Fig. 4, so that it is viewed vertically down the y axis provides a spatial representation of the distribution of dispersal risk around infested tress in each of the locations, and under assumptions of Strict and Relaxed dispersal behavior, and shows that the at-risk area around infested trees is largest in Worcester, MA. The open centers of the shapes represent the spatial distribution of the lower 90th percentile of dispersal distances

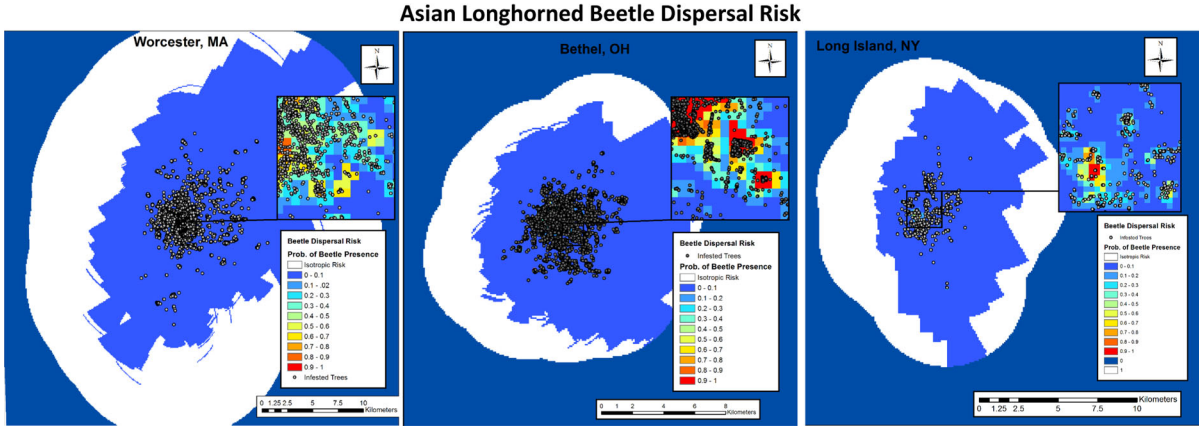

Fig. 6 The application of the dispersal kernel surfaces to each of the landscapes produces a hectare-by-hectare estimate of the probability that at least one beetle has arrived within the hectare, based on the locations and distributions of the infested trees in each landscape. The figures shown provide the estimates of risk for each of the infestations based on the inclusion of anisotropic dispersal, relaxed dispersal behavior, and the low dispersal rate as example outputs. The areas shown in white represent hectares in which there is risk for dispersal under the assumption of isotropic dispersal, but no risk assuming anisotropic dispersal

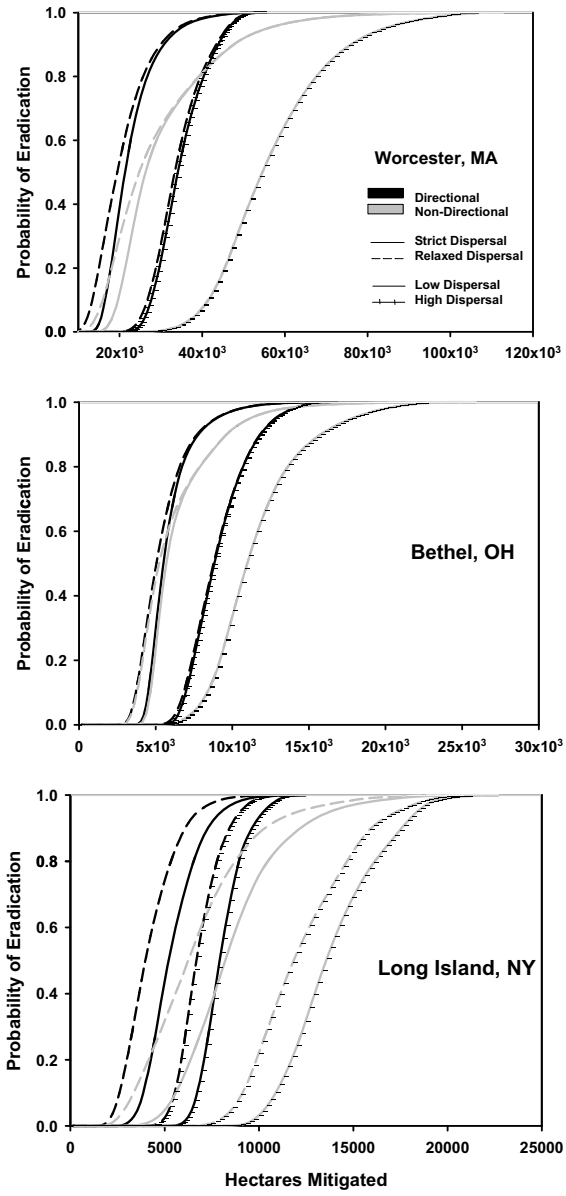

Fig. 7 The curves shown represent the relative effort (measured as the number of hectares on which risk has been mitigated) required to achieve a specified, overall probability of beetle eradication from the landscape. As the curves show, the effort varies among the three infestations, with the required effort being greatest in Worcester, MA. Changes in dispersal behavior (shown by solid and dashed lines) resulted in limited changes in required effort. The inclusion of anisotropic dispersal (black lines) reduced the effort required for eradication when compared to a non-directional distribution of risk (grey lines). Increases in dispersal rate also produced large increases in the effort required for eradication, particularly in the Worcester, MA infestation

by Hull-Sanders et al. (2017) in Worcester, MA found a correlation between apparent long-distance dispersal directions and prevailing wind patterns during the flight season. Within this study the same northeastern bias implied in the Hull-Sanders et al. (2017) study was observed at a larger scale in Worcester, MA, and a preliminary analysis (not shown) suggests long-distance dispersal directions may be related to prevailing wind directions in Bethel, OH. While targeted studies linking these and other patterns remain to be carried out, the availability of dispersal vector distributions from multiple infestations provides a path to explore links between dispersal and weather, and the spatial and temporal scales at which they may operate.

Even without the mechanistic components of anisotropy, the empirical model described here provides a number of advantages over a generalized isotropic distribution of risk. First, the overall perimeter of the at-risk landscape is reduced by excluding dispersal in directions and distances in which dispersal has not been observed. Including this anisotropy survey efforts may benefit from the identification of low-risk areas where the return on investment may be limited, while providing a tool to help ensure that high-risk regions are not under-surveyed.

The second key finding is that this analytical approach provides a framework to explore the roles and effects of poorly studied parameters. For example previous research had suggested beetles may be unlikely to disperse from lightly infested trees (Sawyer 2009), yet in Trotter and Hull-Sanders (2015) and this study the distribution of infested trees suggest this assumption may not be parsimonious, based on the increased dispersal distances and distribution patterns this assumption requires. This contrasting evidence suggests this aspect of beetle behavior remains to be adequately quantified and merits further research. However the analyses shown in Fig. 7 indicate that, while this parameter does have a small effect, the magnitude of this effect is very limited, and other parameters such as dispersal rate may be more informative in estimating the distribution of risk on the landscape.

This approach also has utility in providing tools to evaluate other factors that may influence dispersal. For example, a recent study by Shatz et al. (2016) found relationships between early patterns of dispersal in

Worcester, MA, and distance to forest and spatial distributions of mean annual temperature. Identifying links between these findings with the tools described here may provide a way to asses these patterns at multiple scales and in multiple landscapes. The variations among the wooded-urban-to-contiguous-forest landscape found around Worcester, the fragmented agricultural landscape around Bethel, and the heavily urbanized landscape with limited and widely distributed host trees found on Long Island, may also suggest additional unidentified landscape characteristics that influence Asian longhorned beetle dispersal.

Although this approach offers new utilities and opportunities, it also includes several key limitations driven by model assumptions including; sex ratios, the number of adult beetles produced by trees, the assumption of a homogeneous landscape, the assumption of a fixed dispersal rate, and the absence of a time component. For some of these assumptions, the solutions may be conceptually simple. For example the assumption of a 1:1 sex ratio within beetle populations can be addressed through additional population analyses, and the estimated number of adult beetles produced by each tree could be refined by including precise counts of the exit holes as trees are surveyed, though adding this data collection requirement may include additional costs to survey programs.

The use of homogeneous landscapes to estimate landscape risk, like those shown in Fig. 6 also limits the interpretation of the results. Under real-world conditions the landscape includes a complex matrix of host and non-host regions, dispersal barriers and corridors, and variations in host quality and suitability. By assuming the landscape is entirely suitable the analyses shown here are likely to substantially overestimate the total number of hectares with risk, and further development of these tools should incorporate spatial data (open water, host distribution, etc.). Within the context of this study however the effects of this assumption may be limited. The primary goal was to develop a tool to apply dispersal kernel surfaces to the landscape based on the locations of known infested trees, and to assess the relative impact of multiple parameters on the distribution and intensity of dispersal risk. Using the same standardized landscape for each scenario allows direct comparisons of these parameters both within and among populations.

Some parameters such as dispersal rate require complex, ecologically structured frameworks to address. Within these analyses the effect of dispersal rate was quantified using multiple values, but within each analysis the value was assumed to be fixed. Under field conditions emigration by individual beetles is likely driven by interacting factors such as host quality, mate-finding success, gender, disturbance, and intra-specific interactions which change over time and space. Recent work by Keena et al. (in review) suggests that perceived sex ratios and gender-specific interactions among beetles influence their tendency to take flight. Past work has also shown that beetle density (Bancroft and Smith 2005) and host condition (Keena and Major 2001) play a role in dispersal rates. Capturing dynamic patterns such as beetle density and host condition will require integrating time into the analyses. In its current form the model used can provide estimates of dispersal distances and probabilities, but without time these are not readily converted to rates of spread. Integrating voltanism rates, which are known to vary across the landscape (Trotter and Keena 2016; Kappel et al. 2017), may help to address this limitation.

While the results of these analyses are based on the inclusion of numerous assumptions and should be used with caution, they also represent the synthesis of available knowledge of Asian longhorned beetle dispersal. The approach captures variation within local populations of the beetle and provides both a way to assess the ecological patterns of dispersal, and the distribution of risk which may of use to eradication programs. By continuing to incorporate new information about Asian longhorned beetle as it becomes available, the accuracy of these estimates should continue to improve.

Acknowledgements We thank Robyn Rose, Josie Ryan, Sean Redmond, Phillip Baldauf, and Edward Chen with the United States Department of Agriculture, Animal and Plant Health Inspection Service for assistance in accessing the necessary data, and for helpful comments on the manuscript. We also thank the many surveyors, without their efforts these analyses would not be possible.

References

Bancroft JS, Smith MT (2005) Dispersal and influences on movement for *Anoplophora glabripennis* calculated from individual mark-recapture. Biol Invasions 116:83–92

Favaro R, Wichmann L, Ravn HP, Faccoli M (2015) Spatial spread and infestation risk assessment in the Asian

longhorned beetle, *Anoplophora glabripennis*. Entomol Exp Appl 155:95–101

Haack RA, Poland TM, Gao R-T (2000) The United States experience with the exotic Cerambycid *Anoplophora glabripennis*: Detection, Quarantine, and Control. Silvotecna 14:1–12

Haack RA, Herard F, Sun JH, Turgeon JJ (2010) Managing invasive populations of Asian longhorned beetle and citrus longhorned beetle: a worldwide perspective. Ann Rev Entomol 55:521546

Hull-Sanders H, Pepper E, Davis K, Trotter RT III (2017) Description of an establishment event by the invasive Asian longhorned beetle (*Anoplophora glabripennis*) in a suburban landscape in the northeastern United States. PLoS ONE 12(7):e0181655

Javal M, Roux G, Roques A, Sauvard D (2017) Asian longhorned beetle dispersal potential estimated in computer-linked flight mills. J Appl Entomol 142:282–286. https://doi.org/10.1111/jen.12408

Kappel AP, Trotter RT, Keena MA, Rogan J, Williams CA (2017) Mapping of the Asian longhorned beetle's time to maturity and risk to invasion at contiguous United States extent. Biol Invasions 19:1999–2013. https://doi.org/10.1007/s10530-017-1398-0

Keena M, Major III W (2001) *Anoplophora glabripennis* (*Coleoptera*: *Cerambycidae*) flight propensity in the laboratory. In: Fosbroke SLC, Gottschalk KW (eds) Proceedings, US Department of Agriculture interagency research forum on gypsy moth and other invasive species 2001. Annapolis, MD, USDA Forest Service General Technical Report NE-285, p 81

Keena MA, Moore PM (2010) Effects of temperature on *Anoplophora glabripennis* (Coleoptera: Cerambycidae) larvae and pupae. Environ Entomol 39:1323–1335

Liebhold AM, Tobin PC (2008) Population ecology of insect invasions and their management. Annu Rev Entomol 53:387–408

Lingafelter SW, Hoebeke ER (2002) Revision of *Anoplophora* (Coleoptera: Cerambycidae). Entomological Society of Washington, Washington

Lopez VM, Hoddle MS, Francese JA, Lance DR, Ray AM (2017) Assessing flight potential of the invasive Asian longhorned beetle (Coleoptera: Cerambycidae) with computerized flight mills. J Econ Entomol 110:1070–1077. https://doi.org/10.1093/jee/tox046

Lowe S, Browne M, Boudjelas S, De Poorter M (2000) 100 of the worlds worst invasive species a selection from the Global Invasive Species Database. Invasive Species Specialist Group, Species Survival Commission, World Conservation Union. www.issg.org/booklet.pdf

Meng PS, Trotter RT, Keena MA, Baker TC, Yan S, Schwartzberg EG, Hoover K (2014) Effects of pheromone and plant volatile release rates and ratios on trapping *Anoplophora glabripennis* (Coleoptera: Cerambycidae) in China. Environ Entomol 43:1379–1388

Nehme ME, Trotter RT, Keena MA, McFarland C, Coop J, Hull-Sanders HM, De Moraes CM, Mescher MC, Hoover K (2014) Development and evaluation of a trapping system for *Anoplophora glabripennis* (Coleoptera: Cerambycidae) in the United States. Environ Entomol 43:1034–1044. https://doi.org/10.1603/EN14049

New Jersey Department of Agriculture (NJDA) (2013) New Jersey declares itself free from devastating tree-killing pest. http://www.state.nj.us/agriculture/news/press/2013/approved/press130314.html. Accessed 2 Mar 2017

Peng J, Liu Y (1992) Iconography of forest insects in Hunan China. Hunan Forestry Department/Institute of Zoology, Academia Sinica

Sawyer AJ (2009) Expected dispersal of Asian longhorned beetles from preferred host trees as a function of infestation level and date of removal during the flight season. Final report to the ALB Technical Working Group, August 3, 2009. United States Department of Agriculture, Animal and Plant Health Inspection Service, Plant Protection and Quarantine, Center for Plant Health Science and Technology, Otis Laboratory

Shatz AJ, Rogan J, Sangermano F, Miller J, Elmes A (2016) Modeling the risk of spread and establishment for Asian longhorned beetle (*Anoplophora glabripennis*) in Massachusetts from 2008–2009. Geocarto International 31:813–831. https://doi.org/10.1080/10106049.2015.1086901

Smith MT, Bancroft J, Li G, Gao R, Teale S (2001) Dispersal of *Anoplophora glabripennis* (Cerammbycidae). Environ Entomol 30:1036–1040

Smith MT, Tobin PC, Bancroft J, Li G, Gao R (2004) Dispersal and spatiotemporal dynamics of Asian longhorned beetle (Coleoptera: Cerambycidae) in China. Environ Entomol 33:435–442

Straw NA, Fielding NJ, Tilbury C, Williams DT, Cull T (2016) History and development of an isolated outbreak of Asian longhorn beetle *Anoplophora glabripennis* (Coleoptera: Cerambycidae) in southern England. Agric For Entomol 18:28–293

Trotter RT III, Hull-Sanders HM (2015) Quantifying dispersal of the Asian longhorned beetle (*Anoplophora glabripennis*, Coleoptera) with incomplete data and behavioral knowledge. Biol Invasions 17:3359–3369

Trotter RT III, Keena MA (2016) A variable-instar climate-driven individual beetle-based phenology model for the invasive Asian longhorned beetle (Coleoptera: Cerambycidae). Environ Entomol 45:1360–1370

Turgeon JJ, Orr M, Grant C, Wu Y, Gasman B (2015) Decade-old satellite infestation of *Anoplophora glabripennis* Motschulsky (Coleoptera: Cerambycidae) found in Ontario, Canada outside regulated area of founder population. Coleopt Bull 69:674–678

United States Department of Agriculture (USDA) Animal and Plant Health Inspection Service (APHIS) (2008) USDA and its partners declare victory over Asian longhorned beetle Illinois is first state to reach eradication of the invasive pest. http://www.usda.gov/wps/portal/usda/usdahome?contentid=2008/04/0104.xml. Accessed 2 Mar 2017

United States Department of Agriculture (USDA) Animal and Plant Health Inspection Service (APHIS) (2014a) USDA Declares a Boston, Massachusetts Area Free of the Asian Longhorned Beetle May 12, 2014. https://www.aphis.usda.gov/aphis/newsroom/news/SA_By_Date/SA_2014/SA_05/CT_alb_boston Accessed 12 Feb 2018

United States Department of Agriculture (USDA) Animal and Plant Health Inspection Service (APHIS) Plant Protection

and Quarantine (PPQ) (2014b) Asian Longhorned Beetle Eradication Program, Asian longhorned beetle response guidelines, September 2014. https://www.aphis.usda.gov/plant_health/ea/downloads/2015/alb-eradication-program-eis.pdf. Accessed 2 Mar 2017

Williams DW, Lee H-P, Kim I-K (2004a) Distribution and abundance of *Anoplophora glabripennis* (Coleoptera: Cerambycidae) in natural *Acer* stands in South Korea. Environ Entomol 33:540–545

Williams DW, Li G, Gao R (2004b) Tracking movements of individual *Anoplophora glabripennis* (Coleoptera: Cerambycidae) adults: application of harmonic radar. Environ Entomol 33:644–649

Wu W, Jiang S (1998) The *glabripennis* species group of the genus *Anoplophora* in China. Acta Entomol Sin 41:284–291

Yan J, Qin X (1992) Anoplophora glabripennis (Motsch.). In: Xiao G (ed) Forest insects in China, 1992, 2nd edn. China Forestry Publishing House, Beijing, pp 455–457